

## INVESTIGATION OF MECHANICAL BEHAVIOR AND SHAPE OPTIMIZATION OF ROOFING SHEETS USING METAMODELS

Alexander Janushevskis, Anatolijs Melnikovs, Janis Auzins

Riga Technical University, Institute of Mechanics, 6, Ezermalas iela, Riga, LV-1006, Latvia

### Abstract

*In this work metamodeling approach is discussed for designing of lightweight steel frames and its roofing sheets utilizing advantages of the stressed skin action. In the first step, the roof construction is accurately investigated in terms of both stability and stiffness by solution of mixed shell-beam FE models. The combinations of loads on the structure are considered in accordance to relevant Eurocodes, with special emphasis on the lateral wind loads. Next, for the purpose of computational time reduction, metamodels are created by recently developed original code KEDRO. Finally, cross-section shape of corrugated sheets subjected to appropriate load combination is obtained by global stochastic search procedure to minimize maximal displacement of structure. The result is compared with standardized trapezoidal sheeting.*

**Key words:** metamodeling, shape optimization, roof sheeting

### 1. INTRODUCTION

#### 1.1. Design of the open plan building

Nowadays, the utilization of metal sheeting for roof of the open plan building has become a common practice (The European Standard EN 1993-1-3); as it allows implementing stressed skin diaphragm design, hence, constructing the roof without bracing. That is why, many building companies have continuous attention to designing of steel structures utilizing advantages of stressed skin action, because the implementation of such approach for the open plan buildings might give considerable savings of material and erection time.

However, in many cases, the structure of roof with trapezoidal sheeting that transmit load on the long sides of the frame to wind bracing is described by simplified analytical or computational model (see Figure 1). In these cases the shallow roof of the building or sheeting (Ahmed, 2003) could be idealized as plate with equivalent properties or even considered as a beam, thereby, different effects of diaphragm behavior are neglected. As a result, for instance, FOS may be overestimated, but the benefits of stressed diaphragm effect, in comparison with common framework, would be unnoticeable.

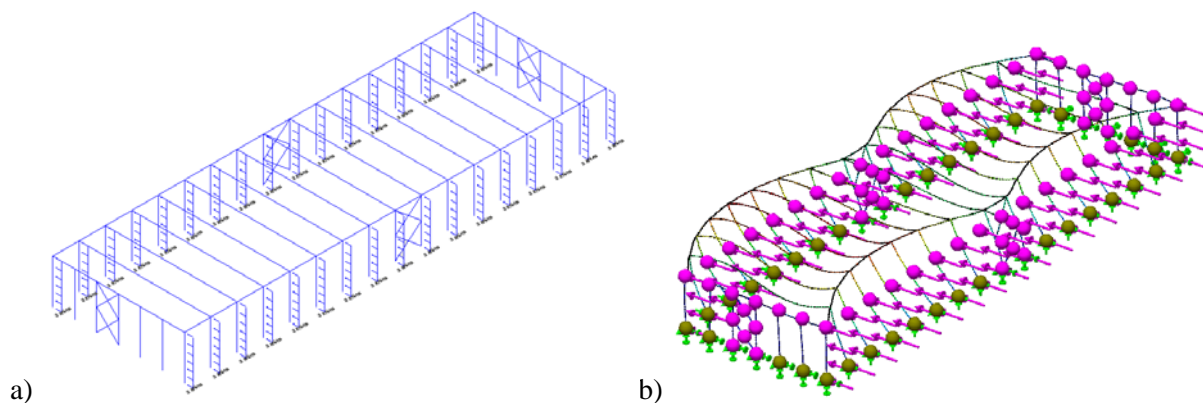


Figure 1. Open plan building with a shallow roof: a) simplified calculation the scheme and b) beam FE model: increased in scale deformations due to side wind load.

On the other hand, complex FE-models are able to describe structural behavior of the roof sheeting together with frame to some extent but such models usually require huge computational resources. Therefore, recession models are desirable in purpose do not sacrifice high accuracy and not carry out whole FE-model calculation for any new parameters sets of the same structure.

### 1.2. FE based structural optimization approaches

In recent years the CAD-based direct parameterization approaches (Saxena & Sahay, 2005) have become highly effective and popular due to rapid development of the integrated CAD/CAE software systems and advanced metamodeling techniques (Lee, 2006), (Simpson, 2004), (Montgomery, 2012), and (Koziel, 2011). NURBS utilization for the freeform curves representation of CAD models can give even more advantages for those techniques. Also references to the kriging based optimization methods (Rasmussen & Williams 2005) and (Sacks, 1989) are commonly given to solve deterministic optimization problems. For non-deterministic structural optimization problems, which account for uncertainties, the optimization is usually based on double loop approaches where the uncertainty propagation is recursively performed inside the optimization iterations. Often the uncertainty estimation for the given point is based on a metamodel, thus allowing reduction of computational time but introducing additional bias in the estimates. In the work (Janusevskis, 2013) a single loop kriging based method for minimizing the mean of an objective function is proposed: simulation points are calculated in order to simultaneously propagate uncertainties, i.e., estimate the mean objective function, and optimize this mean. The choice of this method is appropriate, when optimization of structures with uncertain loading, such as wind loads, must be performed.

For topology and shape optimization of structures the different realizations of homogenization method are vastly used (Arora, J. S. 2004) and (Bendsoe & Sigmund 2003). This method is highly effective for shell constructions. The basic idea of this method is to consider each FE of the mechanical system model as a composite consisting of material and void. The ratio of material volume to void is sought in the FE to maximize the defined criteria, for example, the following performance indicator:

$$PI = \frac{\sigma_{0,max} v_0}{\sigma_{i,max} v_i} \quad (1)$$

where  $\sigma_{0,max}$  is the maximum equivalent stress value of the original design,  $v_0$  a design starting volume, and  $\sigma_{i,max}$  and  $v_i$  the values of variables obtained in the  $i$ -th iteration.

This method was successfully applied for optimization of the automotive industry objects made from isotropic material (Vanderplaats, 2004). However it is very time consuming procedure because number of the design parameters can reach million and more. In the case of solid bodies it frequently produces shapes that are difficult to manufacture. As shown in the work (Mullerschon, 2010) the Hybrid Cellular Automata method does not allow parallelization of computations and PBS queuing system has been used.

### 1.3. Current shape optimization approach and its implementation in KEDRO software

The shape optimization approach based on metamodeling (Janushevskis, 2012) and (Janusevskis, 2013) is used to reduce necessary time and other resources. It includes following 6 steps:

a) Planning the position of the control polygon of non-uniform rational B-splines (NURBS) which can define curves for creating smooth shapes of 3D object in CAD environment. Coordinates of the position of these points are independent variables or factors for design of experiments (DOE). The interval boundaries or side constraints of factors are chosen in accordance with appropriate object size, constructive and technological possibilities or other important considerations. The variables domain should include possible optimal solution, otherwise optimization process must be repeated in loop, adjusting interval boundaries for factors.

- b) Creating of geometrical models of 3D object using CAD software in conformity with DOE. During this step it is possible obtain volume, mass and other inertial characteristics of model that could be used for optimization.
- c) Calculating of responses for complete FEM model using CAE software. This model of object must ensure sufficient accuracy for responses.
- d) Creating metamodels (also called surrogate models) for responses obtained in previous step on the basis of experiment. Accuracy of approximations and prediction errors must be estimated. If results are satisfactory, then proceed with the next step, otherwise try to improve metamodel accuracy.
- e) Using metamodels for shape optimization, i.e. extremum of subsequent objective function is searched by global stochastic search procedures taking into account known constraints.
- f) Validating the optimal design using CAE software for the complete FEM model. Optimal values of factors are used for creation of the optimal shape of 3D object model in CAD software.

The implementation of such approach is available using software KEDRO (Auzins, 2014) that was originally developed as a collection of non-gradient-based optimization tools in Machine and Mechanism Dynamics Research Lab of Riga Technical University. It also includes additional related methods and tools for statistical data sampling, approximation and metamodel-based multiobjective optimization.

## 2. ANALYSIS OF THE ROOF SHEETING BEHAVIOR

The stability and stiffness of the building is considered in term of the roof sheeting behavior under different load combinations.

### 2.1. Stressed skin action in the building with a shallow roof

The building is usually stabilized by wind bracing at the ends of its long sides, so roof sheeting is to transmit loads in normal direction of its profile to the rigid frames in their own planes. The proposed 3D-model is significantly reduced in scale (only 2.6x1.5x4.54 m) in comparison with hangar structures. It consists of beam frames and sheeting (Figure 2a), nevertheless, allows capturing diaphragm behavior of the roof (Figure 3). Also the beam frames is constant during the calculations but sheeting is variable.

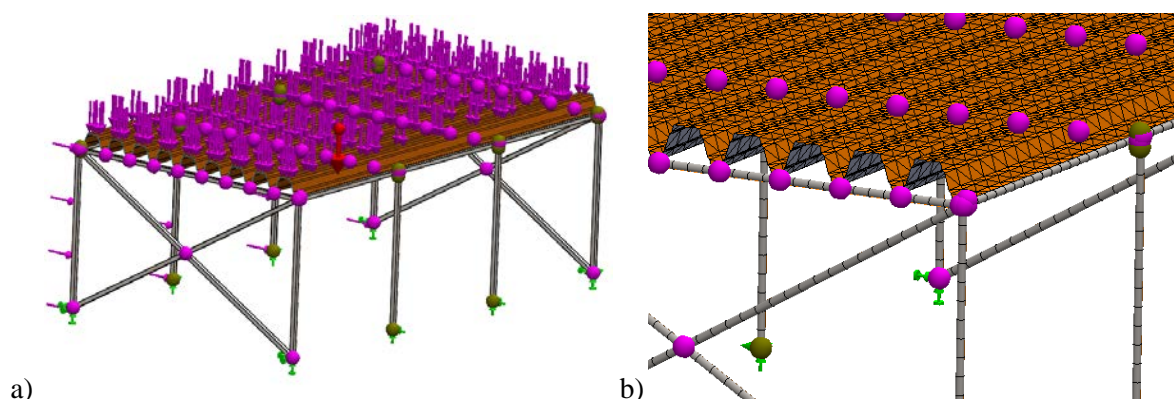


Figure 2. The open plan building with a shallow roof: a) stabilized by wind bracing and b) its FE model.

There are many combinations of loads and loads proportion that might act on the structure, however, when behavior of the roof sheeting is a crucial factor (The European Standard EN 1990), subsequent loads proportion could be assumed (1 - for side wind and 0.6 - for snow load) as well as structure self-weight. The total wind load 18 kN acts normal to long side plane of structure and is uniformly applied to the 4 beams (Figure 2a), and the load from snow acts in normal direction to the roof plane and is

distributed on the sheeting. The self-weight is defined by vertical gravity  $g=9.81\text{m/s}^2$  and material density of the structure elements.

The mixed shell-beam FE is used to reduce the number of DOF (Figure 2b). Thus, the roof sheeting is considered as shell surfaces with constant 0.5 mm thickness. The profiles of frames are square tubing except I-beam under the sheeting; these are meshed by beam elements. The behavior of fasteners of sheeting is not investigated in this study. The joints between profiles and sheeting are defined as bonded contacts zones: they are represented as spheres on the sheeting (Figure 2). These spheres also show joint points of beams. The columns in the corners are fixed at the base but others are rigidly connected as a two-hinged frame.

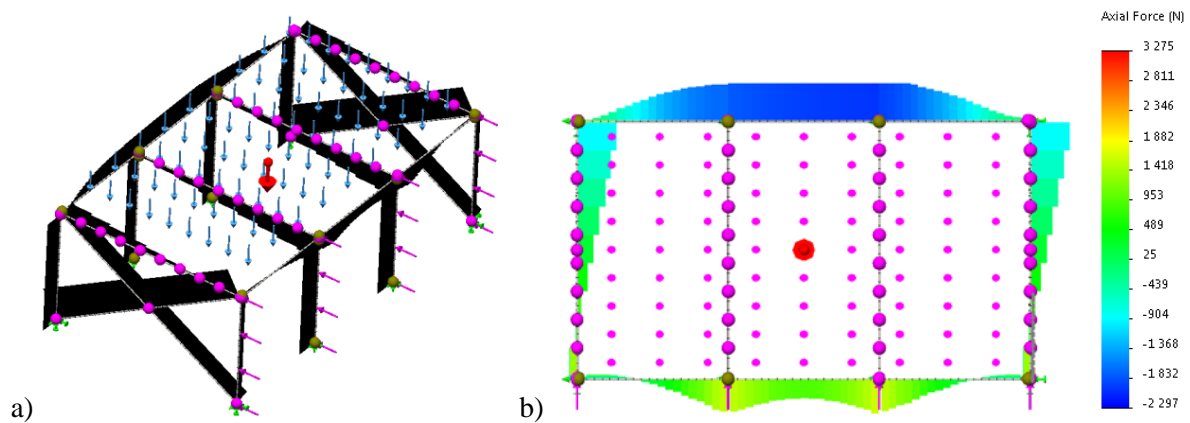


Figure 3. Stressed skin action in FE –model (sheeting is hidden): a) magnitude of axial force in beams and b) in top view.

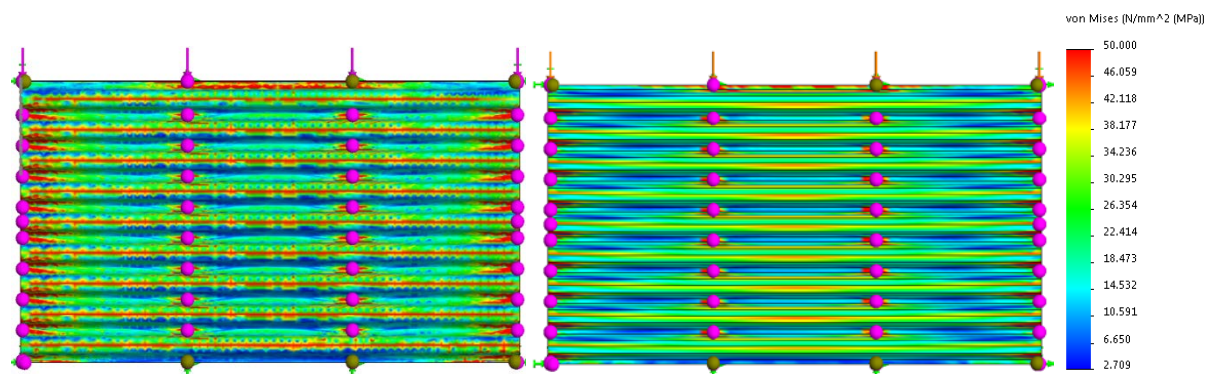


Figure 4. Equivalent stress distribution in the diaphragm with sheets attached to rafters: (1) trapezoidal T153 (right) and sheeting (2) “shaped by NURBS” (left).

The results of the strength calculation are presented on the Figure 3 and 4. The behavior of the proposed model is in close agreement with stressed skin action in building with a shallow roof (Hoglund, 2002). As we can see the roof frame acts to some extent as a deep beam on its side (Figure 3b): the side, where wind force is applied, is subjected to tension but opposite - to compression. In addition, symmetric reaction forces appear from the ends in 2 columns in the corners. The sheeting is stressed (Figure 3a) transmitting loads to the sides wind bracing, where significant axial forces appear.

The equivalent stress distribution in sheeting is demonstrated on the Figure 4, where two designs of sheeting are compared. The trapezoidal sheeting (1) (see profiles on Figure 10) has most of the stress concentrations in areas around fasteners, while stresses in sheeting (2) are more uniformly distributed through the profile.



2.2. Buckling analysis of the sheeting

To utilize correctly the stressed skin action for open plan buildings, the design of the roof must also be checked for buckling effects in the sheeting due to possible combination of loads. Thereby, as the diaphragm behavior may appear in the lower buckling modes of sheeting, and it could significantly contribute to structure stability and integrity. Thus, FEM buckling analysis should be only considered as effective tool for detailed solution of such problem, especially, when accurate representation of buckling modes is required. Moreover, the sheeting of the roof commonly is intended to transmit loads on the long sides to the end, the compression forces is to take place in the one side of the roof frame as was demonstrated on the Figure 3.

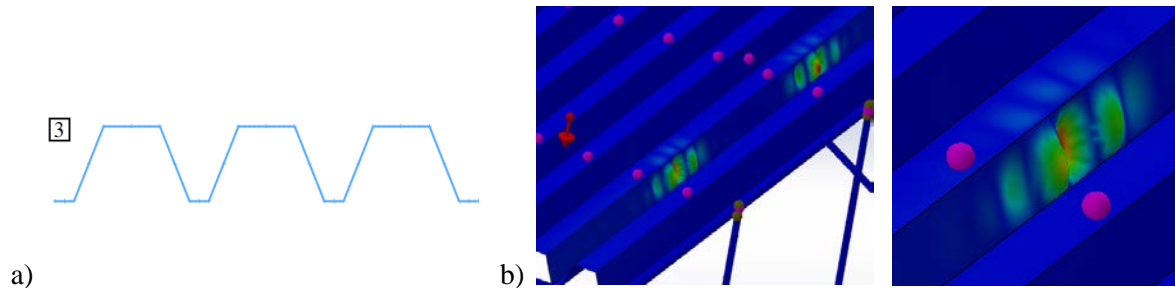


Figure 5. Trapezoidal sheeting of the roof a) cross-section view and b) the first mode of local buckling.

Table 1. Buckling factor of safety (BFS).

Buckling mode	Sheeting type		
	(1) Trapezoidal T153 (Figure 10)	(2) “shaped by NURBS” (Figure 10)	(3) Trapezoidal without ribbing (Figure 5a)
1	5.8944	5.2039	0.56212
2	5.9236	5.4128	0.56338
3	6.0842	5.6712	0.56709
4	6.1947	5.8922	0.56998

If  $0 < \text{BFS} < 1$  then structure buckling is predicted

That is why the profile was checked for load combinations: self-weight + side wind + snow on the roof. The trapezoidal sheeting is assumed without any additional ribs or bends in the cross-section (Figure 5a). FE calculations have been carried out to find the worst scenario. On the Figure 5b the result of case is shown, where self-weight was taken into account together with side load of wind on the structure. This study indicates, that such profile with its relatively big flat faces cannot stand efficiently against compression forces along profile cross-section, and as a result, buckling effects occur in structure (see case (3) in Table 1). This result well complements with behavior of sheeting (Hoglund, 2002), where the local buckling effect is captured: dome shaped displacement along the sheeting flat faces with inverse direction of neighboring domes. In addition, in publication (Mezzomo, 2010) is shown, that such behavior of sheeting could appear in the first or second buckling mode, depending on the loading and boundary conditions.

However, this effect does not occur in sheeting with specially designed shapes, for instance (Figure 10 (1)), where ribs and bends are added in such way so possibility of local buckling due to appropriate

loads is minimized. Also more smooth shape of cross-section (Figure 10 (2)) obtained using NURBS is more effective solution when main problem is to avoid local buckling of sheeting. The BFS for all 3 cross-sections shapes of sheeting are compared in the Table 1. As we can see, the trapezoidal sheeting (3) cannot resist acting load in any considered mode. The (1) sheeting show the best performance, but (2) must take up to ~5 times bigger load to lose stability in the lateral direction to profile. This effect is called profile shear distortion and usually occurs in trapezoidal profiles as crucial disadvantage of stressed skin design (Davies, 2007).

### 3. SHAPE OPTIMIZATION OF ROOF SHEETING

As was demonstrated in the previous section, the sheeting cross-section could considerably affect stability and strength of the structure. Therefore, optimal cross-section shape should be found if advantage of the stressed skin action for the open plan building is to be achieved. For this reason, next, it is proposed using of the previously developed metamodel based approach for shape optimization, because of its effectiveness for shell structures and of easy implementation (Janushevskis, 2014).

#### 3.1. Parameterization of the sheeting cross-section

We start optimization procedure with parameterization of the sheeting cross-section to minimize the number of required parameters to accurately specify shapes of sheeting. Also we want to consider only smooth shapes for profile. Therefore, due to the symmetry of the sheeting cross-section the shape effective parameterization with 4 parameters ( $X_1$ ,  $X_2$ ,  $X_3$  and  $X_4$ ) is proposed, as shown in Figure 6a. The symmetrical half of each element is controlled by control points of a non-uniform rational basis spline (NURBS) polygon. All control points are allowed to move only in X direction, however, the shape of spline is changed in X-Y plane. These parameters are varied in the following ranges:  $70 < X_1 < 130$ ;  $10 < X_2 < 120$ ;  $10 < X_3 < 120$ ;  $70 < X_4 < 130$ , where optimal shape is expected. In addition, control points  $X_1$  and  $X_4$  in this case also define C2 continuity in the connecting points 5 and 1, so for instance, if  $X_4$  is moved away from point 5: the more smooth shape will occur on the span 5-4. When cross-section of sheeting is defined, it is extruded as a surface and then its shape is copied and applied to the whole roof (Figure 6b and c).

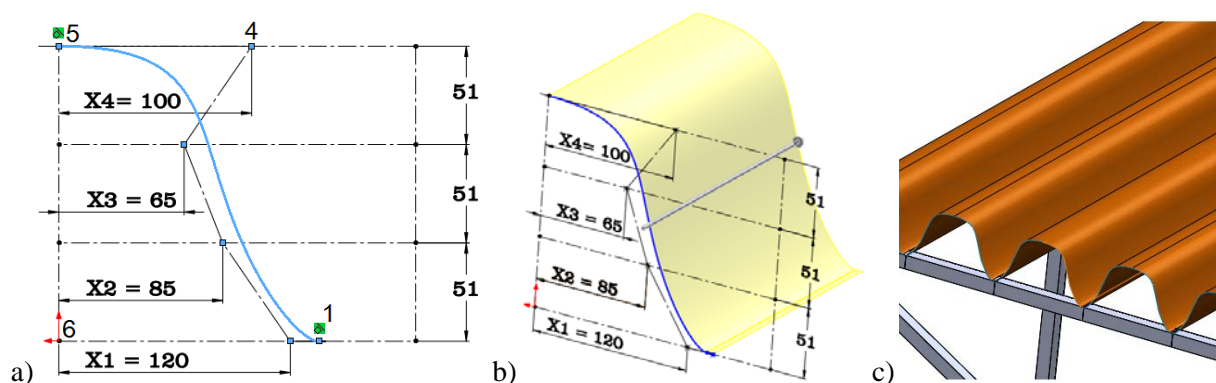


Figure 6. The parameterization of sheeting: a) cross-section shape definition with NURBS polygon points; b) 3D- shape extrusion from plane; and c) result geometry.

#### 3.2. Design of experiments

The design of experiments for 4 factors and 80 trial points (see Figure 7) with mean-square distance (MSD) criterion generated by KEDRO is used. This and many others DOE are available at <http://www.mmd.rtu.lv>.

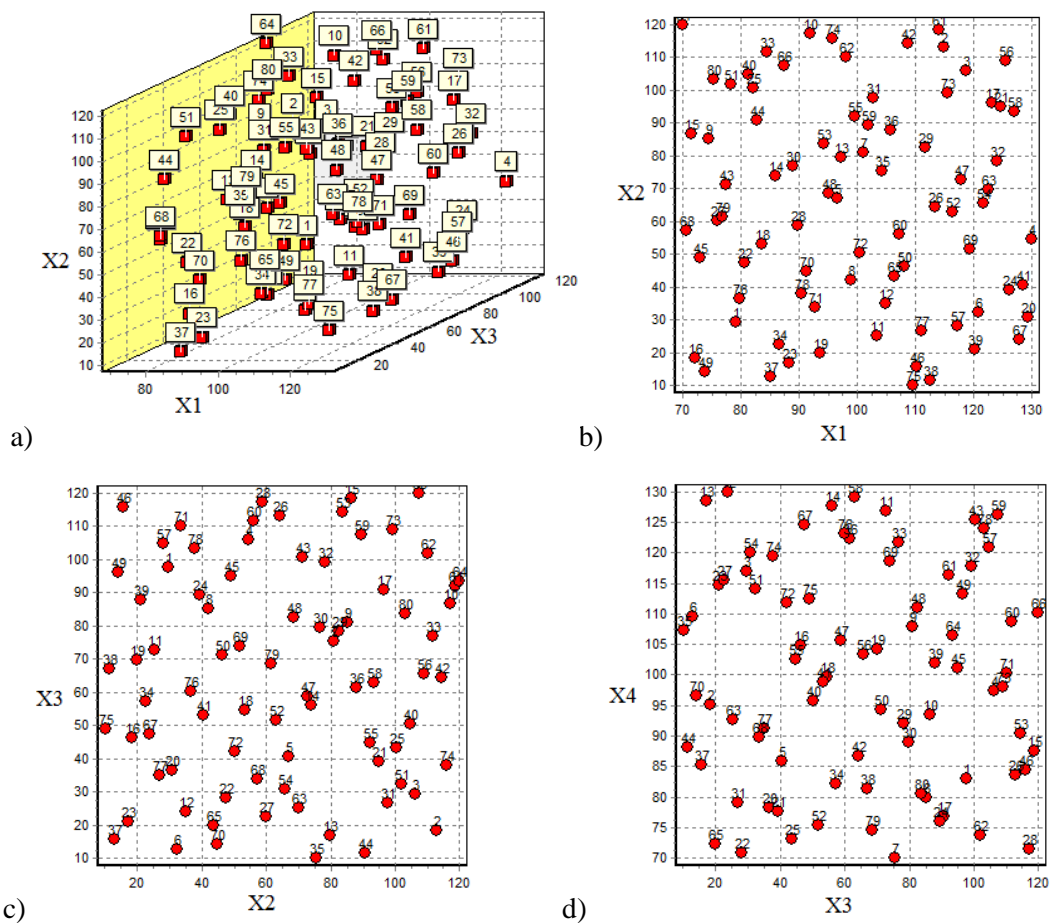


Figure 7. Latin Hypercube DOE (with MSD criterion 0.4120246) for 4 factors and 80 trial points.

The geometrical models of roof sheeting for the structure are developed by CAD software for all variants. In the next step the study from 2.1 section is used for calculation of the responses in accordance to DOE by CAE software SW Simulation. Then these responses are used for approximation by KEDRO. The following expression is used for approximation of response  $y$  by quadratic polynomial:

$$\hat{y} = \beta_0 + \sum_{i=1}^d \beta_i x_i + \sum_{i=1}^{d-1} \sum_{j=i+1}^d \beta_{ij} x_i x_j + \sum_{i=1}^d \beta_{ij} x_i^2 + \varepsilon \quad (2)$$

where there are  $d$  variables  $x_1, \dots, x_d$ ,  $L=(d+1)(d+2)/2$  unknown coefficients  $\beta$  and the errors  $\varepsilon$  are assumed independent with zero mean and constant variance  $\sigma^2$ . In case of local approximation coefficients  $\beta = (\beta_1, \beta_2, \beta_3, \dots, \beta_L)$  depend on point  $x_0$  where prediction is calculated and are obtained by using weighted least squares:

$$\beta = \arg \min_{\beta} \sum_{j \in N_x} w(x_0 - x_j) \times (y_j - \hat{y}(x_j))^2 \quad (3)$$

where the significance of neighboring points in the set  $N_x$  is taken into account by Gaussian kernel:

$$w(u) = \exp(-\alpha u^2) \tag{4}$$

where  $u$  is Euclidian distance from  $x_0$  to current point and  $\alpha$  is coefficient that characterizes significance.

Quality of approximation is estimated by crossvalidation relative error:

$$\sigma_{err} = 100\% \frac{\sqrt{\frac{1}{n} \sum_{i=1}^n (\hat{y}_{-i}(x_i) - y_i)^2}}{\sqrt{\frac{1}{n-1} \sum_{i=1}^n (y_i - \bar{y})^2}} \tag{5}$$

where root mean squared prediction error stands in numerator and mean square deviation of response from its average value stands in denominator,  $n$  is a number of confirmation points and  $\sum_{i=1}^n \hat{y}_{-j}(x_i)$  denotes sum of responses calculated without taking into account  $j$ -th point. Leave one out crossvalidation method is used for calculation of (5).

Functions Yi	1 URES	2 MASS
Sigma Cross	0.207822	0.003969
Sigma Cross%	16.991177%	1.265110%
R2 adjusted	0.980962	0.999890
F-Crit 99%	199.740 > 2.563	35142.660 > 2.563
Sigma	0.168766	0.003287
Sigma%	13.798000	1.047606
MeanExpValue	14.700436	9.249502
StDev of Exp	1.223120	0.313737
Exp. Range	6.029000	1.412200
MaxError	0.259245	-0.005243
Bad Point No.	7	13
Max Rel Error	1.78%	0.06%
BadRelPointNo.	7	13
Max Cook Dist.	-0.561416	-0.007887
Suspicious point	58	6
No.ofActualExp	55	55

Figure 8. Quality indices for approximations of responses.

The quality indices of approximations obtained by KEDRO are shown in Figure 8 for the responses  $y$ : 1 is maximal displacement URES of the roof structure and 2 is the mass of sheeting fragment with standard dimension 560x153x2500 mm. As we can see the accuracy of approximation for the model responses are different. The best value of crossvalidation SigmaCross% (5) is obtained for the mass of sheeting. The mass does not depend on accuracy of the FEA, only from ability to capture the shape of sheeting that is created by NURBS. The response 1 strongly depends on the FEA accuracy. Also, as is demonstrated on the cross-section graphs (Figure 9), the response 1 has more complex dependence from the factors in comparison with 2, that have nearly linear character. Hence as a result, the response 1 requires more sophisticated approximation to be utilized.



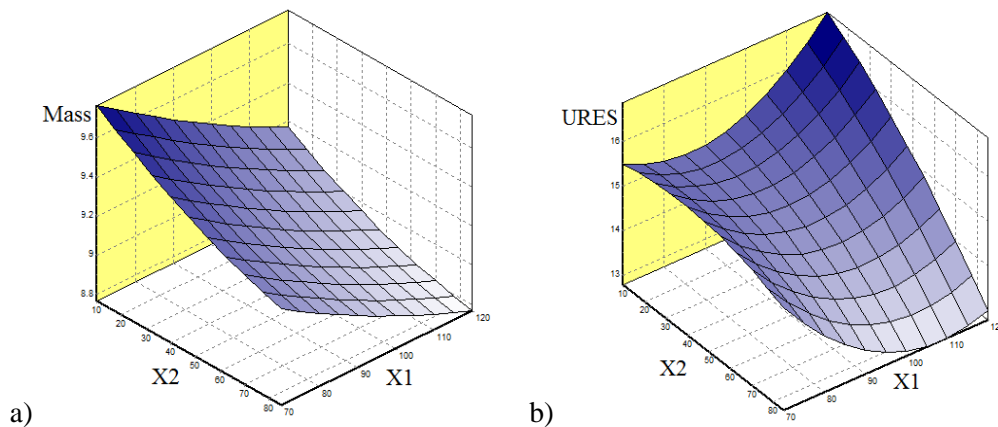


Figure 9. Obtained functional dependences on design variables X1 and X2: a) relative mass of sheeting and b) maximal displacement of the structure.

### 3.3. Optimization of roof sheeting

Next, the prepared metamodels are used for the shape optimization of the sheeting. Problem is defined as follows: minimize the maximal URES displacement of the structure in factors domain range.

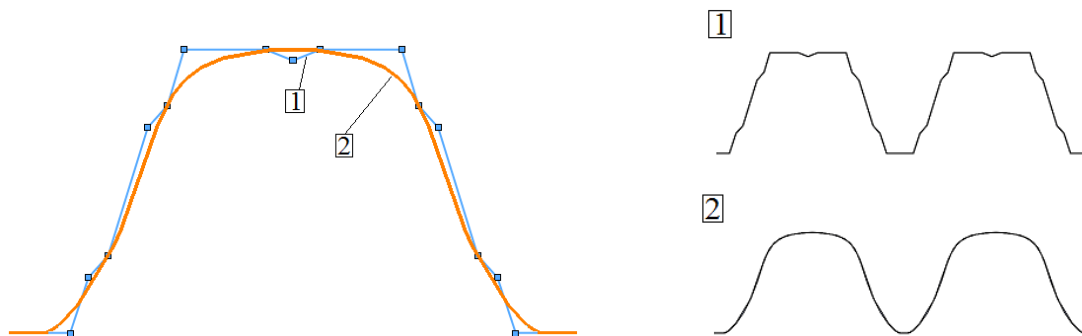


Figure 10. The cross-section of reference (trapezoidal T153) (1) and obtained shape of sheeting (2).

Table 2. The results of sheeting shape optimization.

		Trapezoidal sheeting T153(1)	Obtained shape(2)
X1		-	120.03
X2		-	85.06
X3		-	63.21
X4		-	98.19
URES, mm	metamodels	-	8.51
	actual	8.396	8.236
Mass, kg	metamodels	-	8.671
	actual	9.5045	8.6903

Using locally weighted polynomial approximations of responses and global stochastic search procedure (Janushevskis, 2004), realized in KEDRO, the optimal shape of the roof sheeting is obtained. The smooth shapes of the sheeting is shown and compared with trapezoidal on the Figure 10 and Table 2.

#### 4. CONCLUSIONS

The cross-section of the roofing sheet was successfully optimized using metamodeling approach and competitive solution was introduced and compared with existing trapezoidal sheeting.

The result of buckling analysis has proved that there are no local buckling effects in obtained smooth cross-sections shape of roofing sheeting due to crucial factor of lateral loads.

#### 5. ACKNOWLEDGMENT

This work has been supported by the European Social Fund within the Project No. 2013/0025/1DP/1.1.1.2.0/13/APIA/VIAA/019 “New “Smart” Nanocomposite Materials for Roads, Bridges, Buildings and Transport Vehicle”.

#### REFERENCES

- Ahmed E. & Badaruzzaman, W.H.W. 2003, ‘Equivalent elastic analysis of profiled metal decking using finite elements method’, *Steel Structure*, vol. 3, pp. 9-17.
- Arora, J S 2004, *Introduction to Optimum Design*, 2nd ed., Elsevier, Amsterdam.
- Auzins, J, Janushevskis, A, Janushevskis, J, Skukis, E. 2014, ‘Software EDAOpt for experimental design, analysis and multiobjective robust optimization’, *Proceedings of OPT-i: 1st International Conference on Engineering and Applied Sciences Optimization*, Kos, Greece, pp. 1055-1077.
- Bendsoe, MP & Sigmund, O 2003, *Topology Optimization: Theory, Methods and Application*, 2nd ed., Springer, Berlin.
- Davies, JM 2007, ‘Development in stressed skin design’, *Thin-Walled Structures*, vol. 44, Elsevier, pp. 1250-1260.
- The European Standard EN 1990:2002: *Basis of Structural Design*
- The European Standard EN 1993-1-3: *Design of steel structures - Part 1-3: General rules - Supplementary rules for cold-formed members and sheeting*
- Hoglund, T 2002, *Stabilisation by stressed skin diaphragm action*, Swedish institute of steel construction, Stockholm.
- Janusevskis, J, & Le Riche, R, 2013, ‘Simultaneous kriging-based estimation and optimization of mean response’, *Journal of Global Optimization*, vol. 55, issue 2, Springer, pp. 313-336.
- Janushevskis, A, Akinfiev, T, Auzins, J, Boyko, A 2004, ‘A comparative analysis of global search procedures’, *Proceedings Estonian Acad. Sci. Eng.*, vol.10, No.4, pp. 235-250.
- Janushevskis, A, Auzins, J, & Melnikovs, A, 2012, ‘Shape optimization of mechanical components of measurement systems’, in Z Haq (ed.), *Chapter 12 in Open Access Book “Advanced Topics in Measurements”*, InTech, pp. 243-262.
- Janushevskis, A, Melnikovs, A & Janusevskis J 2014, ‘Robust shape optimization of composite structure using metamodels’, *Proceedings of 4th International Conference on Engineering Optimization ( EngOpt 2014)*, Lisbon, Portugal, pp. 715-721.

Koziel, S, Ciaurri, DE, & Leifsson, L 2011, 'Surrogate-Based Methods', *Computational Optimization, Methods and Algorithms*, Springer, Berlin, pp. 33 -59, 2011.

+Lee, TH, Jung, JJ 2006, 'Metamodel-based Shape Optimization of Connecting Rod Considering Fatigue Life', *Key Engineering Materials*, VOL 306/308, pp. 211-216.

Mezzomo, G.P, Iturrioz, I, Grigoletti, G, Gomes H.M. 2010, 'Investigation of the mechanical behavior of trapezoidal roofing sheets using genetic algorithms', *Expert System with Application*, vol. 37, Elsevier, pp. 939-948.

Montgomery, DC 2012, *Design and Analysis of Experiments*, 8th ed, Wiley, New York.

Mullerschon, H, Lazarov, N, & Witowski, K 2010, 'Application of Topology Optimization for Crash with LC-OPT/Topology', *Proc. 11th Int LS-DYNA Users Conference*, pp.17-46.

Rasmussen, CE, Williams, CKI, 2005, *Gaussian Processes for Machine Learning: Adaptive Computation and Machine Learning*, The MIT Press, MIT.

Sacks, J, Welch, JW, Mitchell, JT, Wynn HP, 1989, 'Design and analysis of computer experiments', *Statistical Science*, Nov. 4(4), pp. 409 -423.

Saxena, A, Sahay, B. 2005, *Computer Aided Engineering Design*, Springer, Berlin.

Simpson, TW, Booker, AJ, Ghosh, D, Giunta, AA, Koch, NP, Yang, R 2004, 'Approximation Methods in Multidisciplinary Analysis and Optimization: A Panel Discussion', *Structural and Multidisciplinary Optimization*, vol. 27, pp. 320- 313.

Vanderplaats, GN 2004, *Numerical Optimization Techniques for Engineering Design with Applications*, 4th ed. Vanderplaats Research & Development, Inc. Colorado Springs, Colorado.